TESLA Report 2004-01

Wake Fields Generated by the LOLA-IV Structure and the 3rd Harmonic Section in TTF-II

I. Zagorodnov, T. Weiland

Technische Universität Darmstadt, Darmstadt, Germany

M.Dohlus

Deutsches Elektronen-Synchrotron (DESY), Hamburg, Germany

(Dated: January, 2004)

Abstract

In this report we estimate long- and short-range wake functions for new elements to be used in TESLA Test Facility (TTF) – II. The wake potentials of the LOLA-IV structure and the 3rd harmonic section are calculated numerically for very short bunches and analytical approximations for wake functions in short and long ranges are obtained by fitting procedures based on analytical estimations.

1 INTRODUCTION

In this report we estimate long- and short-range wake functions for new elements to be used in TESLA Test Facility (TTF) – II. The wake potentials of the LOLA-IV structure and the 3rd harmonic section are calculated numerically for very short bunches and analytical approximations for wake functions in short range are obtained by fitting procedures.

The analytical model for short-range wake functions is based on analytical estimations of short range wakes of different elements. It is a combination of terms corresponding to the case of an infinite periodic cavity-like structure, a structure of finite length and the case of a step transition (step collimator).

To estimate the long-range wake function the wake potential for long distance up to 2 meters after the bunch is calculated. It allows to estimate the low frequency spectra of the wake potential and to obtain an analytical form of the long-range wake function.

The numerical results are obtained with code ECHO [1] for high relativistic Gaussian bunches with RMS deviation σ up to 15 μm. The calculations are carried out for the complete structures (including bellows, rounding of the irises and the different end cell geometries) supplied with ingoing and outgoing pipes.

The low frequency spectra of the wake potentials is calculated using the Prony-Pisarenko method [7].

2 LONGITUDINAL WAKE FUNCTION OF LOLA-IV STRUCTURE

The LOLA-IV transverse deflecting cavity has to be used as a diagnostic for measuring the length of very short bunches in the TTF-II.

The LOLA structure consists of 104 cells. The gap g for the middle cells is equal to 29.1338 mm and for the end cells - to 29.0957 mm. The irises with radius $a = 22.4409\ mm$ are rounded and have the thickness 5.842 mm. The initial part of the geometry is shown in Fig 1. The total length of the structure is equal to $\sim 3.6m$.

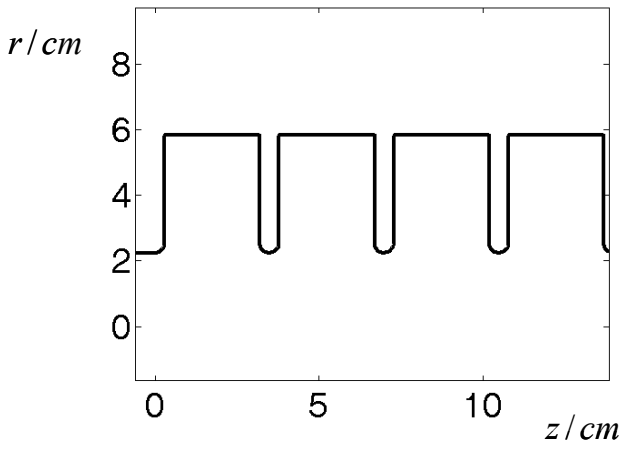

Fig 1. The geometry of the LOLA structure.

The calculated longitudinal wake potentials (solid lines)

$$W_{\parallel}^{0}(s)=\frac{1}{Q}\int_{-\infty}^{s} w_{\parallel}^{0}(s-s')q(s')ds'$$

together with analytical approximations (5) (dashed lines) are shown in Fig. 2.

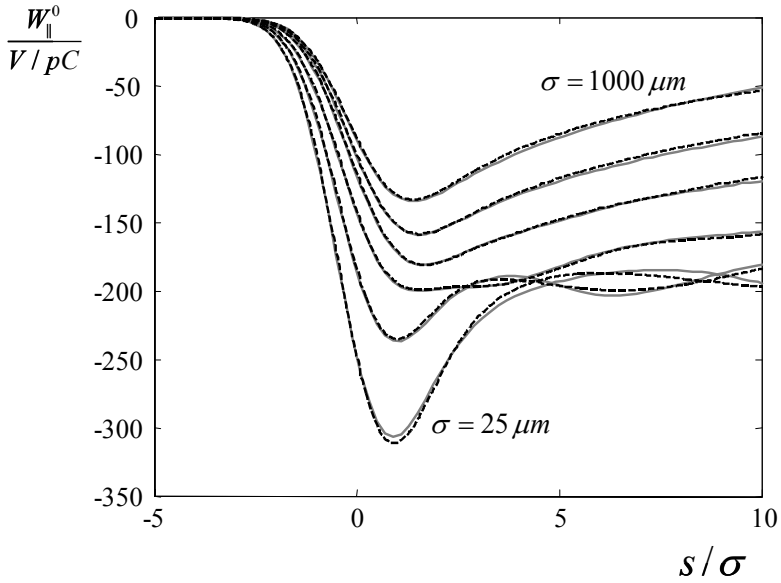

Fig 2. Comparison of numerical (solid lines) and "analytical" (dashed lines) longitudinal wake potentials in the LOLA structure for Gaussian bunches with $\sigma = 25, 50, 100, 250, 500, 1000\,\mu m$.

The LOLA cavity can be treated as a periodic structure of finite length. As shown in Ref. [2] the high frequency behavior of impedance is complicated. The high frequency dependence of impedance for an infinite periodic structure is $\omega^{-3/2}$ that differs essentially from finite structure $\omega^{-1/2}$ behavior. As the LOLA structure has a finite length there is a transition region where the frequency behavior of impedance changes from $\omega^{-3/2}$ to $\omega^{-1/2}$. The above argument explains the complicated oscillated behavior of the wake potentials for the shortest bunches (see Fig.2). To describe the oscillations the one cell solution [3] is modified by a cosine factor preserving the original asymptotic behavior.

To find an analytical approximation of the wake function a fitting process was used. As an analytical model we used a combination of the modified one cell and periodic structure solutions:

$$w_{\parallel}^{0}(s)=-\theta(s)\left[Ae^{-\sqrt{s/s_0}}+B\frac{\cos(\omega s^{\alpha})}{\sqrt{s}+Cs^{\beta}}\right]. \qquad (1)$$

The first term in equation (1) describes a periodic $O(1), s\to 0,$ behavior and as shown in Ref. [2] the first coefficient can be estimated as

$$A=\frac{Z_0 c}{\pi a^2}L_{total}=\frac{Z_0 c}{4\pi}\frac{4}{a^2}L_{total}=8.994\cdot 10^9\frac{4}{0.02244^2}3.6375=260\cdot 10^{12}. \qquad (2)$$

The expression for estimation of the coefficient s_0, suggested in Ref. [3], results in

$$s_0=0.41\frac{a^{1.8}g^{1.6}}{L^{2.4}}=0.41\frac{0.02244^{1.8}\cdot 0.0291338^{1.6}}{(0.005842+0.0291338)^{2.4}}=4.8\cdot 10^{-3}. \qquad (3)$$

The second term in equation (1) should describe a finite structure $O(s^{-0.5}), s\to 0,$ behavior as well as oscillations seen in Fig. 2. As shown in Ref. [4] the coefficient B can be estimated as

$$B = \frac{Z_0 c\sqrt{L_{total}}}{\sqrt{2}\pi^2 a} = \frac{Z_0 c}{4\pi}\frac{2\sqrt{2L_{total}}}{\pi a} = 8.994\cdot 10^9 \frac{2\sqrt{2\cdot 3.6375}}{\pi\cdot 0.02244} = 0.7\cdot 10^{12}\,. \qquad (4)$$

Fitting the wake function in form (1) to the numerical wake potentials shown in Fig.2 the following analytical expression is obtained

$$w_{\parallel}^0(s) = -\theta(s)\left[257.6e^{-\sqrt{\frac{s}{3.96\cdot 10^{-3}}}} + 1.16\frac{\cos(1760s^{0.72})}{\sqrt{s}+1600s^{1.23}}\right]\ \left[\frac{V}{pC}\right]. \qquad (5)$$

The numerical coefficients in Eq. (5) are consistent with approximations (2)-(4).

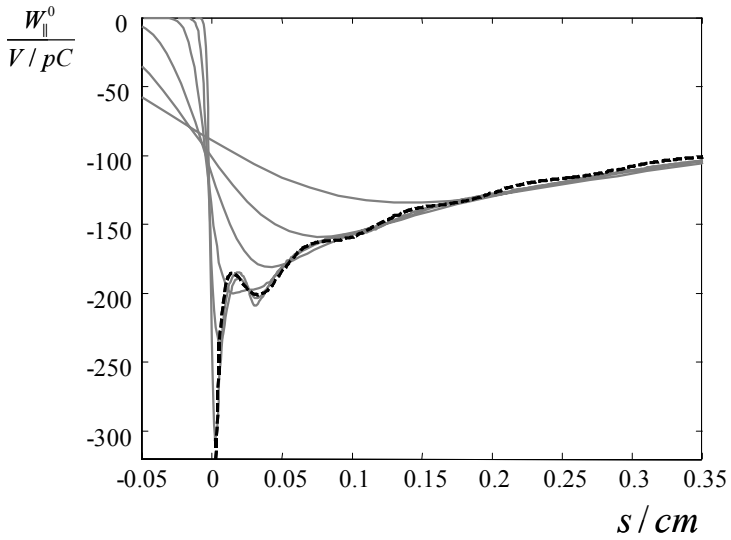

Fig 3. The "analytical" longitudinal wake function (dashed line) for the LOLA structure and numerical (solid lines) wake potentials for Gaussian bunches with $\sigma = 25, 50, 100, 250, 500, 1000\,\mu m$.

Fig. 3 shows wake function (5) together with numerical wake potentials (solid gray lines) outlined earlier in Fig.2. We see that the wake function tends to be an envelope function to the wakes.

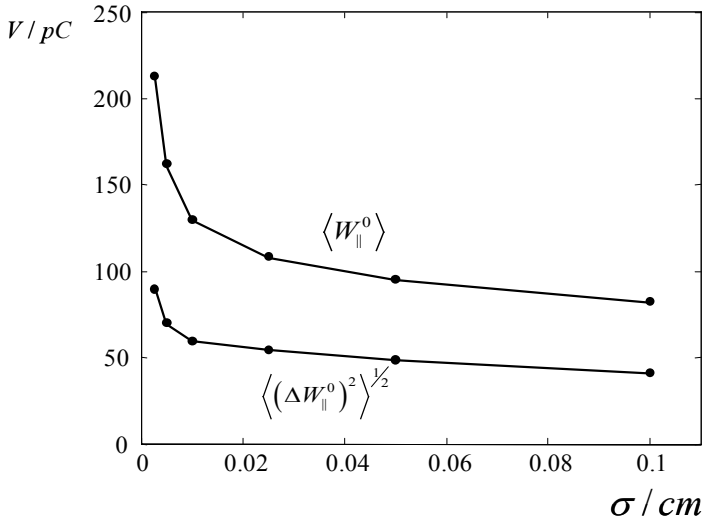

Fig 4. Comparison of numerical (lines) and "analytical" (points) longitudinal integral parameters for the LOLA structure.

Fig. 4 shows the analytical (solid lines) and numerical (points) loss factors and energy spreads for Gaussian bunches with $\sigma = 25,50,100,250,500,1000\mu m$. The coincidence of the results let us use analytical expression (5) as the short range longitudinal wake function.

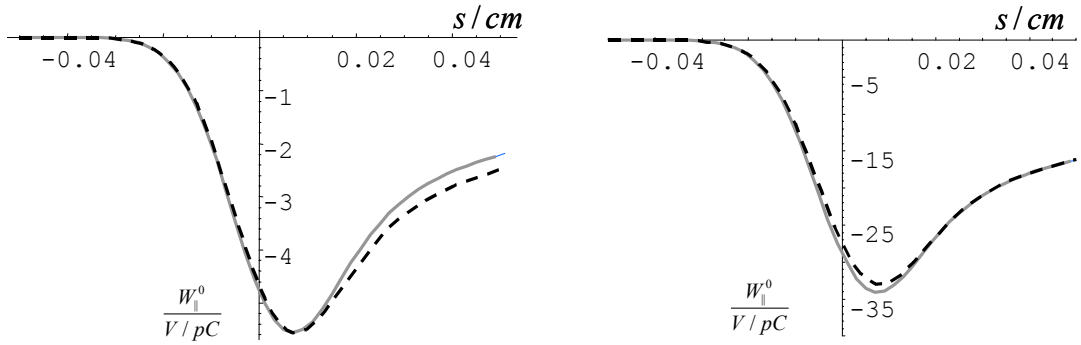

Fig 5. Comparison of numerical (solid line) and "analytical" (dashed line) longitudinal wake potentials for one cell (left) and ten cells (right) of the LOLA structure.

As the next check the above results can be compared to the analytical estimations given in Ref. [5], p.243. The impedance of structure consisting of N pillboxes at the high frequency limit can be estimated by an expression

$$Z_{\parallel}(\omega) = \sum_{k=1}^{N} (Y_1(\omega) + Y_2(\omega,k))^{-1}, \qquad (6)$$

$$Y_1(\omega) = \frac{a\pi}{Z_0 c}\left(1 + i\ sign(\omega)\right)\left(\frac{\pi|\omega|c}{g}\right)^{0.5},$$

$$Y_2(\omega,k) = \frac{1}{Z_0}\alpha\sqrt{k-1}\tan^{-1}\left(\frac{\alpha}{2\sqrt{k}}\right),$$

$$\alpha = (1 + i\ sign(\omega))a\sqrt{\frac{\pi|\omega|}{Lc}}.$$

Fig. 5 shows comparison of the numerical and analytical (6) wake potentials in one and ten middle cells of the LOLA cavity for a bunch with $\sigma = 100\mu m$. Equation (6) is obtained in Ref. [5] for square irises. To take into account weakening of the wake fields due to rounding of irises an effective iris radius $\overline{a} = 1.13a$ is used in calculations and coincidence of the numerical and analytical curves can be seen in Fig. 5.

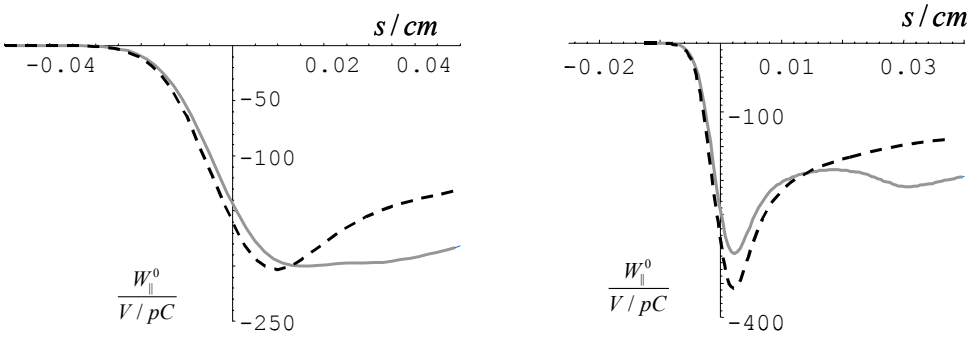

Fig 6. Comparison of numerical (solid line) and "analytical" (dashed line) longitudinal wake potentials for $\sigma = 100\mu m$ (left) and $\sigma = 25\mu m$ (right) in the LOLA structure.

For the complete 104 cells LOLA structure the results are shown in Fig.6 for bunches with $\sigma = 100\mu m$ (left) and $\sigma = 25\mu m$ (right). We see that equation (6) is not able to describe transient behavior presented by cosine term in Eq.(1).

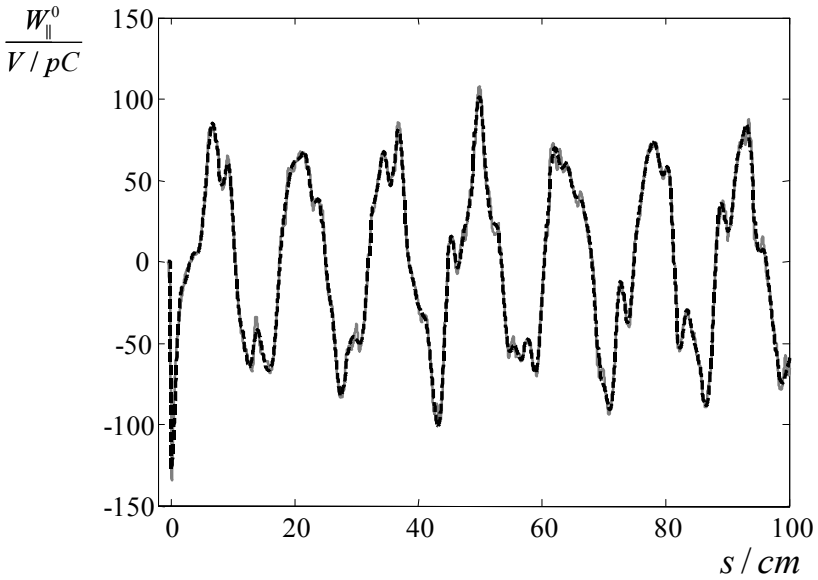

Fig 7. The long-range numerical (solid line) and "analytical" (dashed line) longitudinal wake potentials for Gaussian bunch with $\sigma = 1mm$ in the LOLA structure.

The numerical results were checked by densening of the mesh by factor 2 for Gaussian bunch with $\sigma = 50\mu m$. The wakes for different mesh resolutions coincide graphically and the loss factors are different less than by 0.5%. As the second argument to confirm the accuracy, the closeness of the wake potentials to the envelope function in Fig.3 can be used, because of the mesh for shorter bunch is two times denser as before.

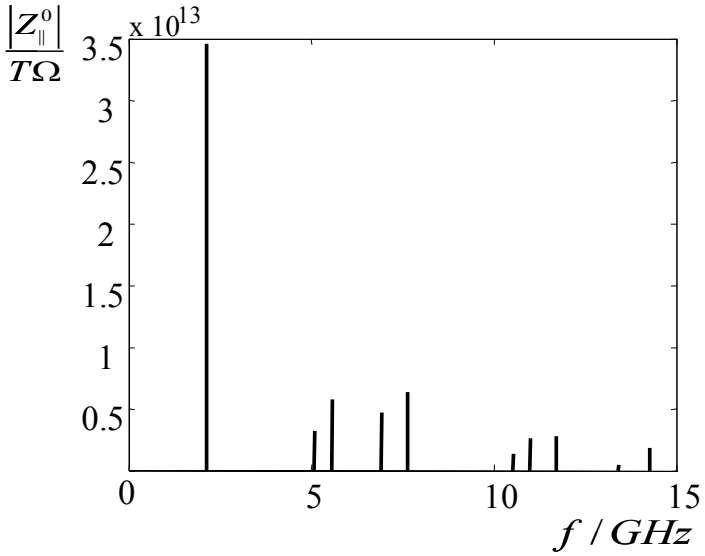

Fig 8. The longitudinal low-frequency impedance in the LOLA structure.

To estimate long range wake fields the wake potential for Gaussian bunch with $\sigma = 1mm$ is calculated for distance up to 2 meter after the bunch. Fig.7 shows numerical

(solid line) and analytical (dashed line) wake potentials up to 1 meter after the bunch.

The longitudinal wake function can be approximated by expression

$$w_{\parallel}(s) = -\theta(s)\left[2\sum_{i=1}^{\infty} K_i \cos(\frac{2\pi}{c} f_i s) + R(s)\right], \qquad (7)$$

where summation over the cavity modes is supplemented by term $R(s)$ because of the pipes on both sides of the structure. To obtain an approximation of the long-range wake function we keep in Eq. (7) only a finite number ($N = 10$) of addends corresponding to the lowest frequencies.

f_i, GHz	2.11	5.09	5.57	6.93	7.62	10.5	11	11.7	13.4	14.3
K_i, 10^{12}	34.6	3.26	5.76	4.7	6.4	1.3	2.6	2.8	0.42	1.8

Table 1. The lowest frequencies and their amplitudes for long-range longitudinal wake function of the LOLA structure.

Fig. 8 shows the frequencies and amplitudes used in Eq. (7) to obtain the wake function shown in Fig.7 by dashed line. The values are obtained using the Prony-Pisarenko algorithm [7] and are given in Table 1. The Prony-Pisarenko algorithm is a method to fit a set of decaying oscillation characterized by amplitudes, phases and damping constants to a given curve or data set and is used in our paper as alternative to the discrete Fourier transform.

3 TRANSVERSE WAKE FUNCTION OF LOLA-IV STRUCTURE

In this section we repeat the exercise for transverse case. The calculated transverse wake potentials (solid lines) together with analytical approximations (dashed lines) are shown in Fig. 9.

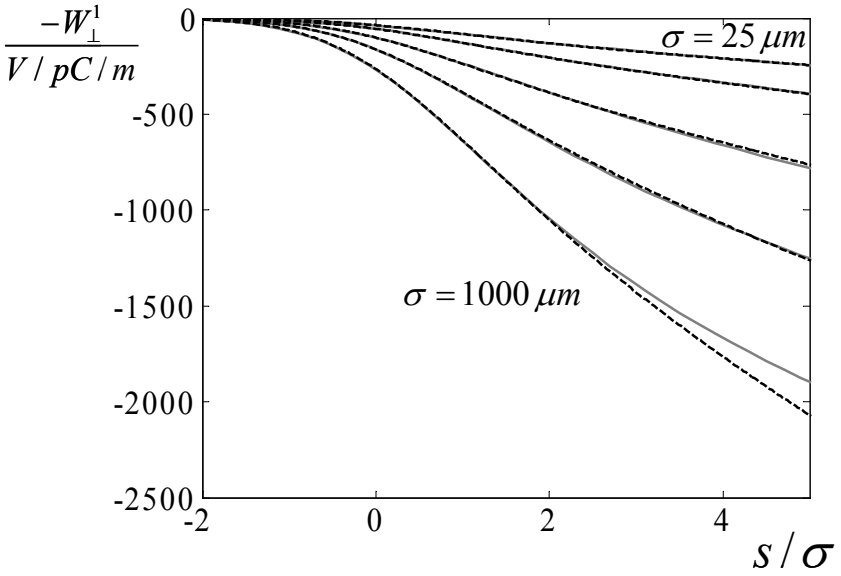

Fig 9. Comparison of numerical (solid lines) and "analytical" (dashed lines) transverse wake potentials for the LOLA structure.

To find an analytical approximation of the wake function a fitting process was used.

As an analytical model we used a combination of the one cell and periodic structure solutions:

$$w_{\perp}^{1}(s) = \theta(s)\left[A s_1 \left(1 - (1 + \sqrt{s/s_1}) e^{-\sqrt{s/s_1}}\right) + B\sqrt{s} \right]. \quad (8)$$

The first term in equation (8) describes a periodic $O(s), s \to 0,$ behavior. The expression for estimation of the coefficient s_1, suggested in Ref. [6], results in

$$s_1 = 0.169 \frac{a^{1.79} g^{0.38}}{L^{1.17}} = 2.4 \cdot 10^{-3}. \quad (9)$$

And as shown in Ref. [6] the first coefficient can be estimated as

$$A s_1 = \frac{2}{a^2} \frac{Z_0 c}{\pi a^2} 2 s_1 L_{total} = 4951 \cdot 10^{12}. \quad (10)$$

The second term in equation (8) should describe a finite structure $O(s^{0.5}), s \to 0,$ behavior. As shown in Ref. [4] the coefficient B can be estimated as

$$B = \frac{2}{a^2} \frac{Z_0 c \sqrt{2 L_{total}}}{\pi^2 a} = 5467 \cdot 10^{12}. \quad (11)$$

Fitting the wake function in form (8) to the numerical wake potentials shown in Fig.9 the following analytical expression is obtained

$$w_{\perp}^{1}(s) = \theta(s)\left[10200\left(1 - \left(1 + \sqrt{\frac{s}{11.7 \cdot 10^{-3}}}\right) e^{-\sqrt{\frac{s}{11.7 \cdot 10^{-3}}}}\right) + 9200\sqrt{s} \right] \left[\frac{V}{pC \cdot m}\right]. \quad (12)$$

The numerical coefficients in Eq. (12) are consistent at least in order with approximations (9)-(11).

Fig. 10 shows wake function (12) together with numerical wake potentials outlined earlier in Fig.9. We see that the wake function tends to be an envelope function to the wakes.

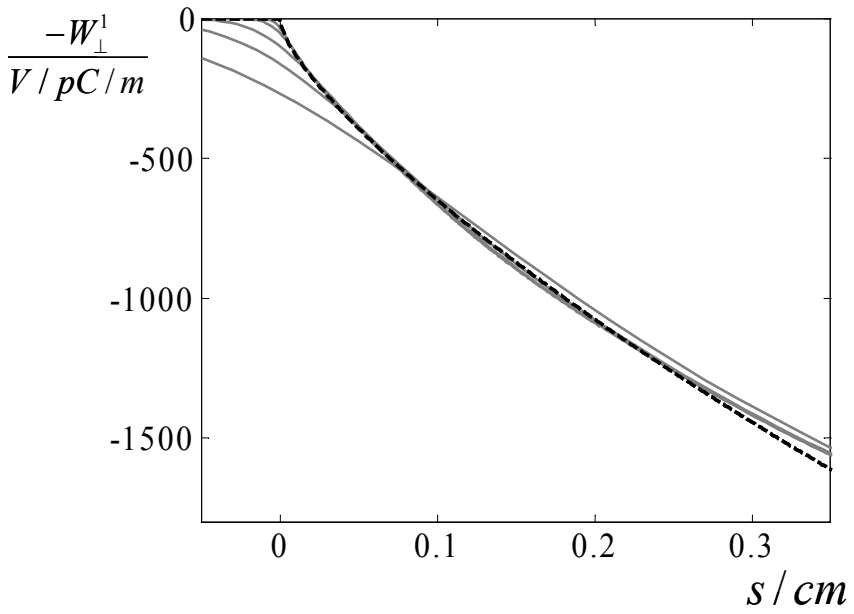

Fig 10. The "analytical" transverse wake function (dashed line) for the LOLA structure and numerical (solid lines) wake potentials for Gaussian bunches with $\sigma = 25, 50, 100, 250, 500, 1000 \mu m$.

Fig. 11 shows the analytical (solid lines) and numerical (points) kick factors and kick spreads. The coincidence of the results let us use the analytical expression (12) as short range

transverse wake function.

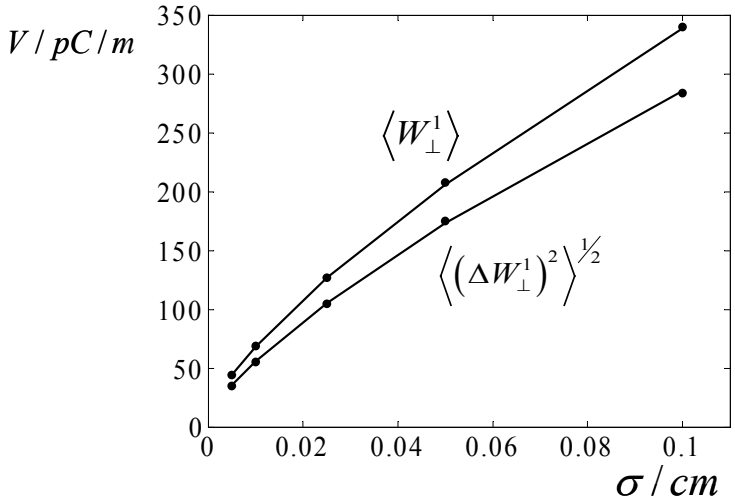

Fig 11. Comparison of numerical (lines) and "analytical" (points) transverse integral parameters for the LOLA structure.

To estimate long range transverse wake fields the wake potential for Gaussian bunch with $\sigma = 1mm$ is calculated for distance up to 2 meters after the bunch. Fig.12 shows numerical (solid gray line) and analytical (dashed black line) wake potentials up to 1 meter after the bunch.

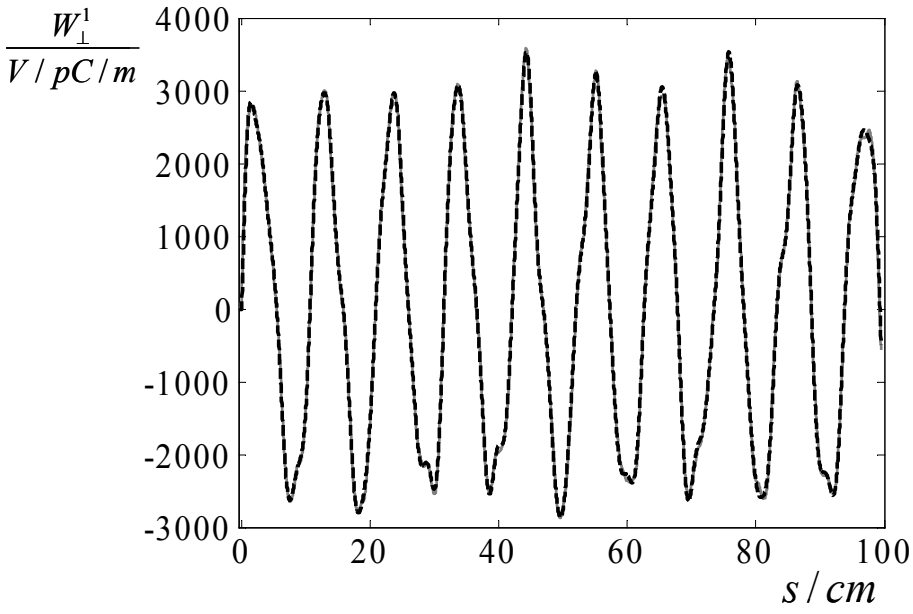

Fig 12. The long-range transverse wake potential for Gaussian bunch with $\sigma = 1mm$ in the LOLA structure. The analytical approximation is shown by black dashed line.

The transverse wake function can be approximated by formula

$$w_{\perp}(s) = \theta(s)\left[2\sum_{i=1}^{\infty} K_i \frac{c}{2\pi f}\cos(\frac{2\pi}{c} f_i s) + R(s)\right]. \qquad (13)$$

To obtain approximation of long-range wake function we keep in the Eq. (13) only finite

number ($N = 12$) of addends corresponding to the lowest frequencies.

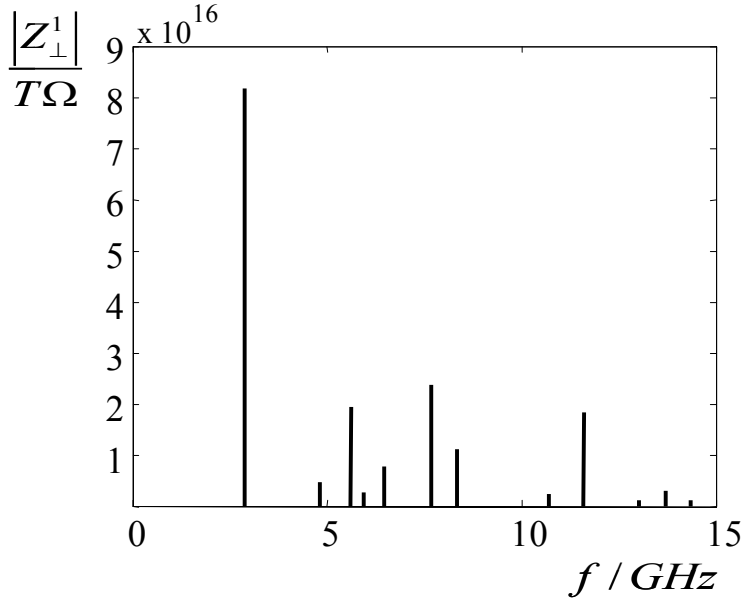

Fig 13. The transverse low-frequency impedance of the LOLA structure.

Fig. 13 shows the frequencies and amplitudes used in Eq. (13) to obtain the wake function shown in Fig.12 by dashed line. The values are obtained using the Prony-Pisarenko algorithm [7] and are given in Table 2.

f_i, *GHz*	2.87	4.81	5.60	5.93	6.45	7.67	8.32	10.7	11.6	13.0	13.7	14.3
K_i, 10^{16}	8.17	0.47	1.94	0.27	0.79	2.38	1.11	0.25	1.87	0.13	0.31	0.12

Table 2. The lowest frequencies and their amplitudes for long-range transverse wake function of the LOLA structure.

4 LONGITUDINAL WAKE FUNCTION OF THE 3RD HARMONIC SECTION

For the phase 2 of the TESLA test facility (TTF 2) it has been planed to use a cavity section operated at three times the 1.3 GHz frequency of the existing TTF1 cavities to compensate nonlinear distortions of the longitudinal phase space. The 3rd harmonic section consists of 4 TESLA-like (but reduced by factor 3) cavities with 13-fold bellows in between. The iris radius is $a = 15\ mm$. The cavities are connected with pipes of the radius $a_p = 20\ mm$. On both ends of the section there are step transitions from a_p to $b = 39mm$ as shown in Fig 14.

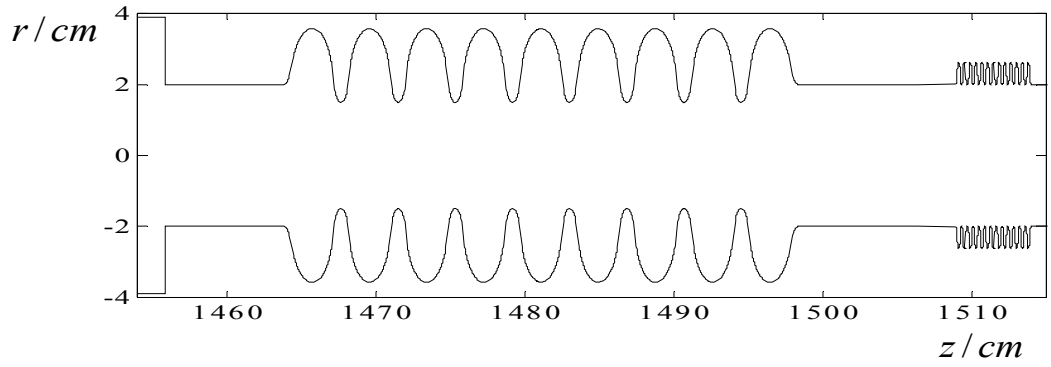

Fig 14. The part of the geometry of the 3rd harmonic section. Only one cavity is shown. The whole structure includes 4 cavities and 3 bellows.

The calculated longitudinal wake potentials (solid lines) together with analytical approximations (dashed lines) are shown in Fig. 15.

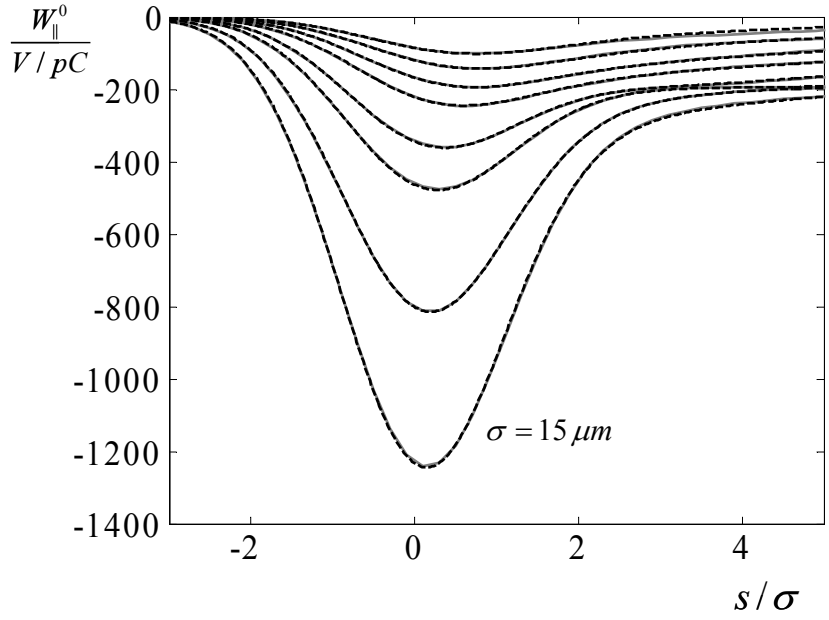

Fig 15. Comparison of numerical and "analytical" longitudinal wake potentials in the 3rd harmonic section for Gaussian bunches with $\sigma = 15, 25, 50, 75, 150, 250, 500, 1000 \mu m$.

Because of the step transitions from a_p to b the model (1) is not sufficient to describe the wake function of the structure and Eq.(1) should be supplemented by an additional term for the step collimator. For a high relativistic bunch, $\gamma \gg 1$, the high frequency impedance of a step collimator does not depend on the frequency and is the following constant [5]

$$Z_{\parallel}(\omega) = \frac{Z_0}{\pi} \ln \frac{a_p}{b},\ \gamma > \frac{\omega}{c} b \gg 1.$$

Hence a Dirac-delta function has to be added to Eq. (1) and it reads

$$w_{\parallel}^0(s) = -\theta(s)\left[Ae^{-\sqrt{s/s_0}} + B\frac{\cos(\omega s^{\alpha})}{\sqrt{s} + Cs^{\beta}} + D\delta(s) \right]. \quad (14)$$

The first term in equation (14) describes a periodic $O(1), s \to 0,$ behavior and can be estimated as

$$A = \frac{Z_0 c}{\pi a^2} L_{total} = \frac{Z_0 c}{4\pi} \frac{4}{a^2} L_{total} = 8.994 \cdot 10^9 \frac{4}{0.015^2} 1.3838 = 221 \cdot 10^{12}. \quad (15)$$

The expression for estimation of the coefficient s_0 results in

$$s_0 = 0.41 \frac{a^{1.8} g^{1.6}}{L^{2.4}} = 0.41 \frac{0.015^{1.8} \cdot 0.0323^{1.6}}{0.03844^{2.4}} = 2.2 \cdot 10^{-3}. \quad (16)$$

The second term in equation (14) is intended to describe the finite structure $O(s^{-0.5}), s \to 0,$ behavior and oscillations. The coefficient B can be estimated as

$$B = \frac{Z_0 c \sqrt{L_{total}}}{\sqrt{2}\pi^2 a} = \frac{Z_0 c}{4\pi} \frac{2\sqrt{2L_{total}}}{\pi a} = 8.994 \cdot 10^9 \frac{2\sqrt{2 \cdot 1.3838}}{\pi \cdot 0.015} = 0.64 \cdot 10^{12}. \quad (17)$$

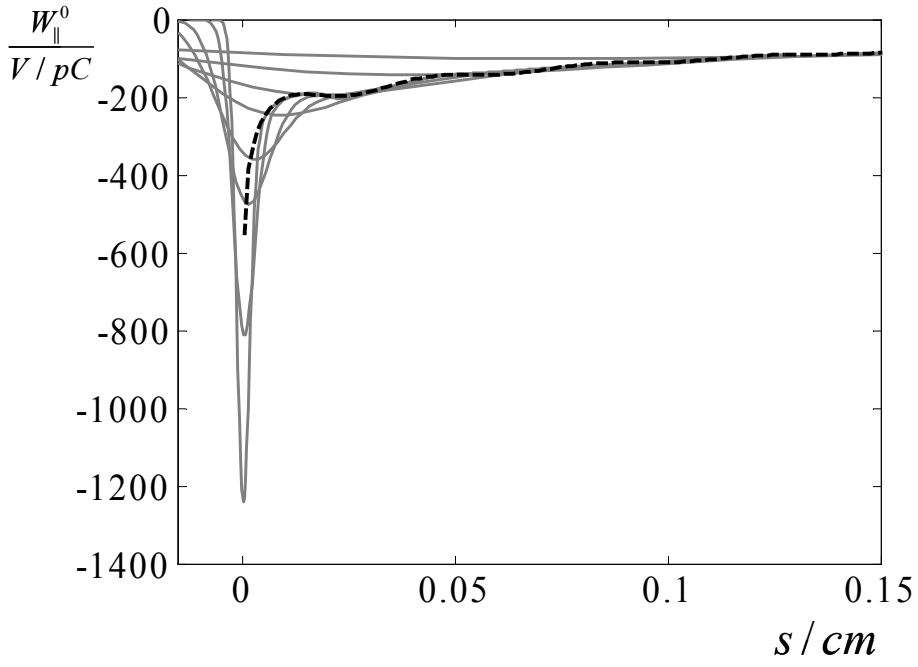

Fig 16. The "analytical" longitudinal wake function of the 3rd harmonic section.

Finally, the last coefficient is

$$D = \frac{Z_0 c}{\pi} \ln \frac{a_p}{b} = 0.024 \cdot 10^{12}. \quad (18)$$

Fitting the wake function in form (16) to the numerical wake potentials shown in Fig.15 the analytical expression is obtained

$$w_{\parallel}^{0}(s) = -\theta(s)\left[318e^{-\sqrt{\frac{s}{8.4\cdot 10^{-4}}}} + 0.9\frac{\cos(5830s^{0.83})}{\sqrt{s}+195s} + 0.036\delta(s) \right]\left[\frac{V}{pC}\right]. \qquad (19)$$

The numerical coefficients A, B, s_0, D in Eq. (19) agree well with approximations (15)-(18).

Fig. 16 shows wake function (19) together with numerical wake potentials outlined earlier in Fig.15.

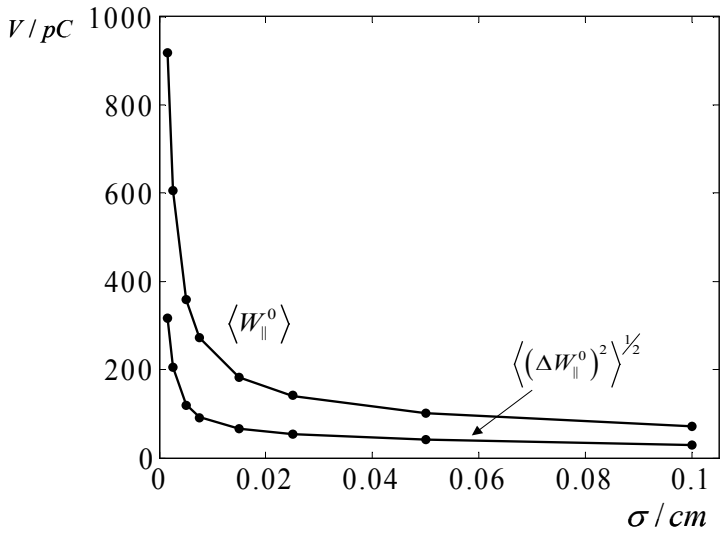

Fig 17. Comparison of numerical (solid lines) and "analytical" (points) longitudinal integral parameters for the 3rd harmonic section.

Fig. 17 shows the analytical (solid lines) and numerical (points) loss factors and energy spreads. The coincidence of the results let us use analytical expression (19) as the short range longitudinal wake function for 3rd harmonic section.

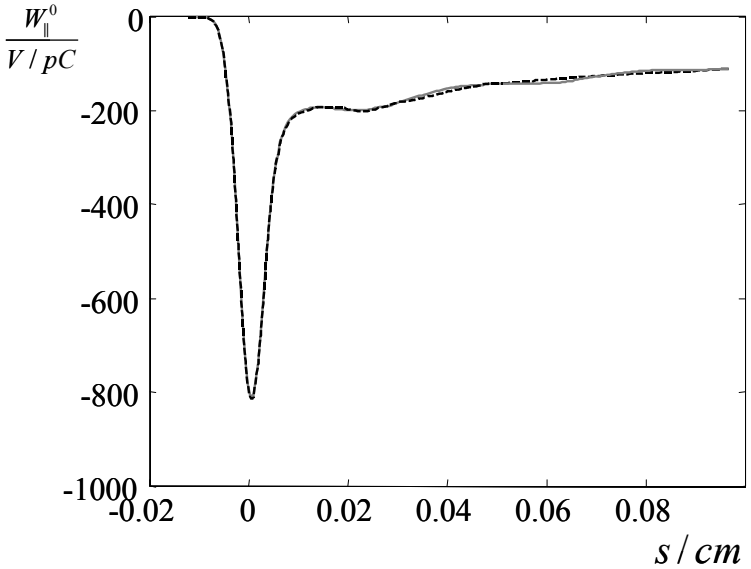

Fig 18. Comparison of numerical (solid line) and "analytical" (dashed line) longitudinal wake potentials for the 3rd harmonic section.

Fig. 18 shows comparison of numerical (solid line) and analytical (19) wake potentials

for bunch with $\sigma = 25\mu m$. We see that formula (19) describes very well the transient behavior available in the numerical solution.

The numerical results are checked by densening of the mesh by factor 2 for Gaussian bunch with $\sigma = 50\mu m$. The wakes coincide graphically and the loss factors are different less than by 0.5%. For example we obtained for bunch with $\sigma = 15\mu m$ the loss factor is equal to 606.5 for the mesh resolution with 5 points on sigma and is equal to 606.2 for the mesh resolution with 5 points on sigma that confirms a high accuracy of the numerical results.

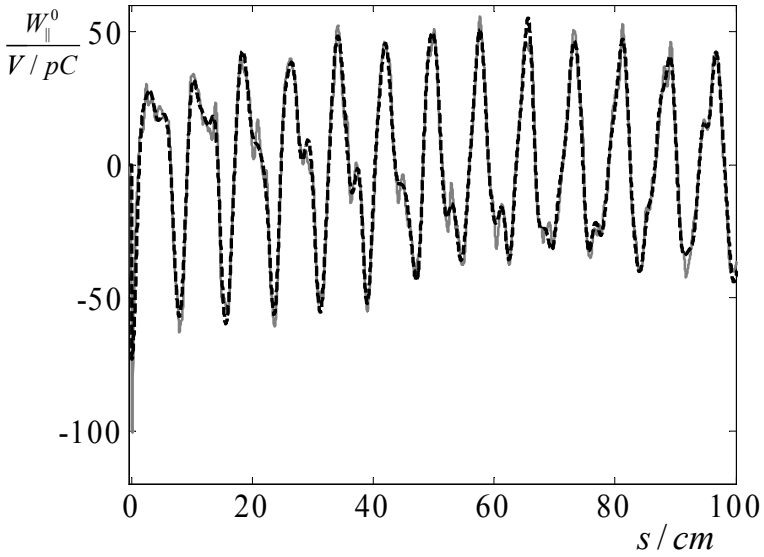

Fig 19. The long-range longitudinal wake potential for Gaussian bunch with $\sigma = 1mm$ in the 3rd harmonic section.

To estimate the long range wake fields the wake potential for a Gaussian bunch with $\sigma = 1mm$ is calculated for distance up to 2 meter after the bunch. Fig.19 shows numerical (solid line) and analytical (dashed line) wake potentials up to 1 meter after the bunch.

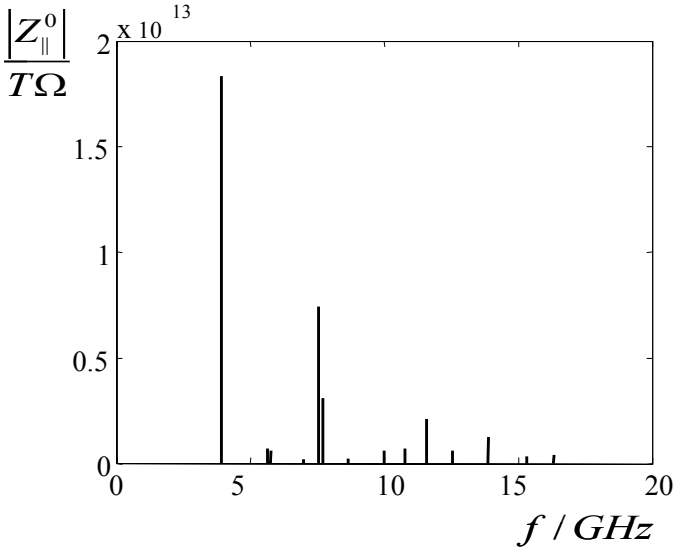

Fig 20. The longitudinal low-frequency impedance for the 3rd harmonic section

To obtain approximation of long-range wake function we keep in the Eq. (7) only a

finite number ($N = 14$) of addends corresponding to the lowest frequencies.

Fig. 20 shows the frequencies and amplitudes used in Eq. (7) to obtain the wake function shown in Fig.19 by dashed line. The values are obtained using the Prony-Pisarenko algorithm and are given in Table 3.

f_i, GHz	3.90	5.65	5.73	6.97	7.54	7.69	8.65
K_i, 10^{12}	18.3	0.73	0.61	0.20	7.44	3.08	0.22

f_i, GHz	9.98	10.7	11.6	12.5	13.9	15.3	16.3
K_i, 10^{12}	0.63	0.72	2.08	0.60	1.25	0.34	0.41

Table 3. The lowest frequencies and their amplitudes for long-range longitudinal wake function of 3rd harmonic section.

5 TRANSVERSE WAKE FUNCTION OF THE 3RD HARMONIC SECTION

The calculated transverse wake potentials (solid lines) together with analytical approximations (dashed lines) are shown in Fig. 21.

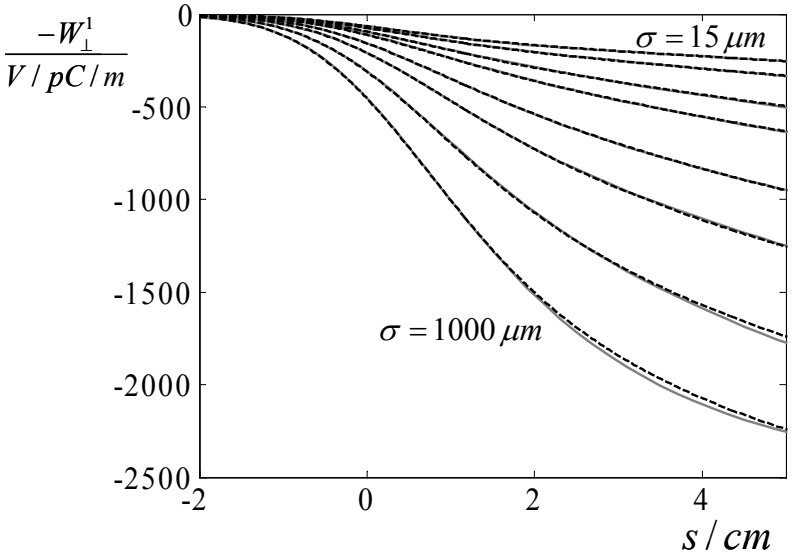

Fig 21. Comparison of numerical and "analytical" transverse wake potentials in 3rd harmonic section for Gaussian bunches with $\sigma = 15, 25, 50, 75, 150, 250, 500, 1000\,\mu m$.

Because of the step transitions from a_p to b the model (8) has to be supplemented by an additional term for the step collimator. If we suggest that the relation [6]

$$Z_\perp(\omega) = \frac{2c}{\omega a^2} Z_\parallel(\omega),$$

which is true at high frequencies for cavity-like structures, holds for collimators too, then a constant has to be added to model (8)

$$w_{\perp}^{1}(s)=\theta(s)\left[\,A s_1\left(1-(1+\sqrt{s/s_1})e^{-\sqrt{s/s_1}}\right)+B\sqrt{s}+C\,\right]. \qquad (20)$$

The first term in equation (22) describes a periodic $O(s), s\to 0,$ behavior. The expression for estimation of the coefficient s_1 results in

$$s_1=0.169\frac{a^{1.79}g^{0.38}}{L^{1.17}}=1.1\cdot 10^{-3}. \qquad (21)$$

And the first coefficient can be estimated as

$$As_1=\frac{4}{a^2}\frac{Z_0 c}{\pi a^2}s_1 L_{total}=4255\cdot 10^{12}. \qquad (22)$$

The second addend in equation (22) is intended to describe a finite structure $O(s^{0.5}), s\to 0,$ behavior. The coefficient B can be estimated as

$$B=\frac{2}{a^2}\frac{Z_0 c\sqrt{2L_{total}}}{\pi^2 a}=11290\cdot 10^{12}. \qquad (23)$$

Finally, the last coefficient is

$$C=\frac{2}{a_p^2}\frac{Z_0 c}{\pi}\ln\frac{a_p}{b}=120\cdot 10^{12} \qquad (24)$$

Fitting the wake function in form (20) to the numerical wake potentials shown in Fig.21 the analytical expression is obtained

$$w_{\perp}^{1}(s)=\theta(s)\left[\,2232\left(1-\left(1+\sqrt{\frac{s}{0.56\cdot 10^{-3}}}\right)e^{-\sqrt{\frac{s}{0.56\cdot 10^{-3}}}}\right)+5441\sqrt{s}+88.5\,\right]\ \left[\frac{V}{pC\cdot m}\right]. \qquad (25)$$

The numerical coefficients in Eq. (25) are consistent at least in order with approximations (21)-(24).

Fig. 22 shows wake function (27) together with the numerical wake potentials outlined earlier in Fig.21. We see that the wake function tends to be an envelope function to the wakes.

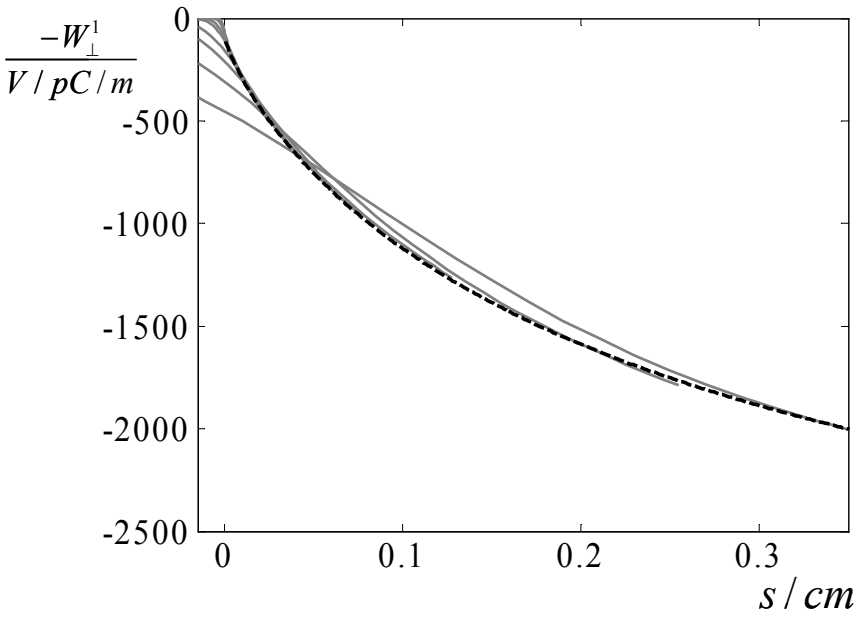

Fig 22. The "analytical" (dashed line) transverse wake function for the 3rd harmonic section and wakes for Gaussian bunches with $\sigma=15,25,50,75,150,250,500,1000\mu m$.

Fig. 23 shows the analytical (solid lines) and numerical (points) kick factors and kick

spreads. The coincidence of the results let us use the analytical expression (25) as the short range transverse wake function of the 3rd harmonic section.

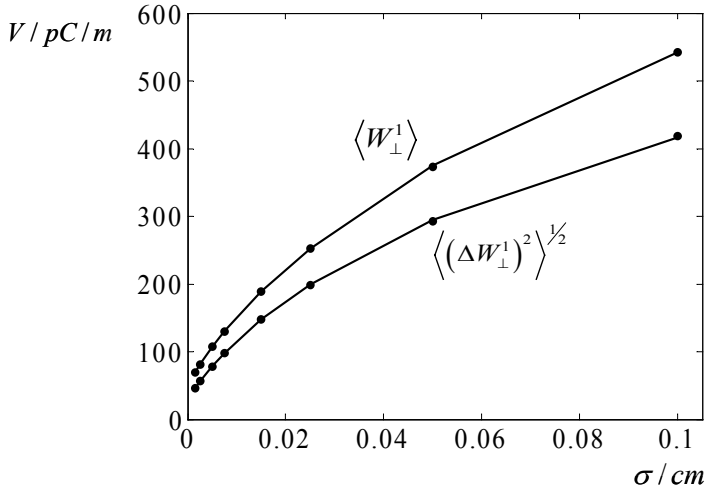

Fig 23. Comparison of numerical (solid lines) and "analytical" (points) transverse integral parameters for the 3rd harmonic section.

To estimate long range transverse wake fields the wake potential for Gaussian bunch with $\sigma = 1mm$ is calculated for distance up to 2 meter after the bunch. Fig.24 shows the numerical (solid line) and analytical (dashed line) wake potentials up to 1 meter after the bunch.

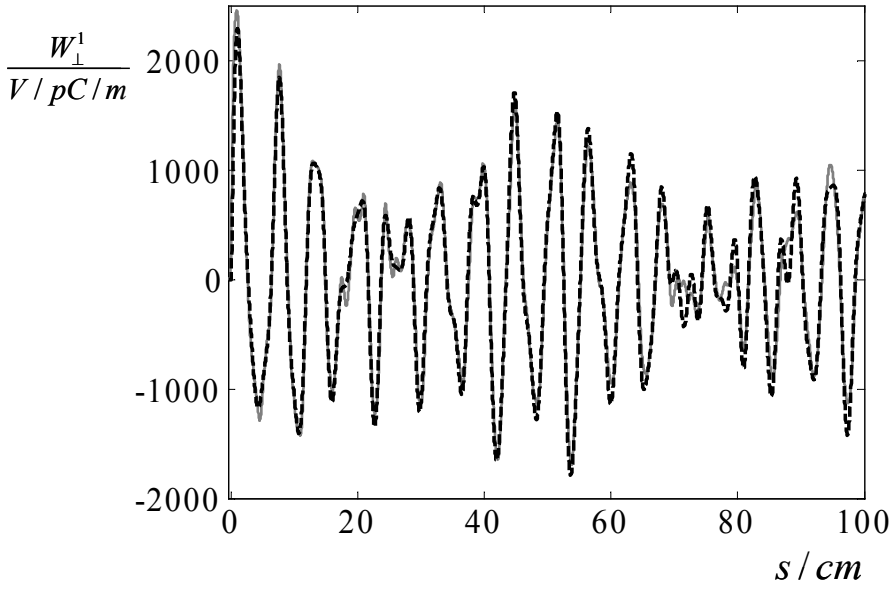

Fig 24. The long-range transverse wake potential for Gaussian bunch with $\sigma = 1mm$ in 3rd harmonic section.

To obtain approximation of long-range wake function we keep in the Eq. (13) only a finite number ($N = 14$) of addends corresponding to the lowest frequencies.

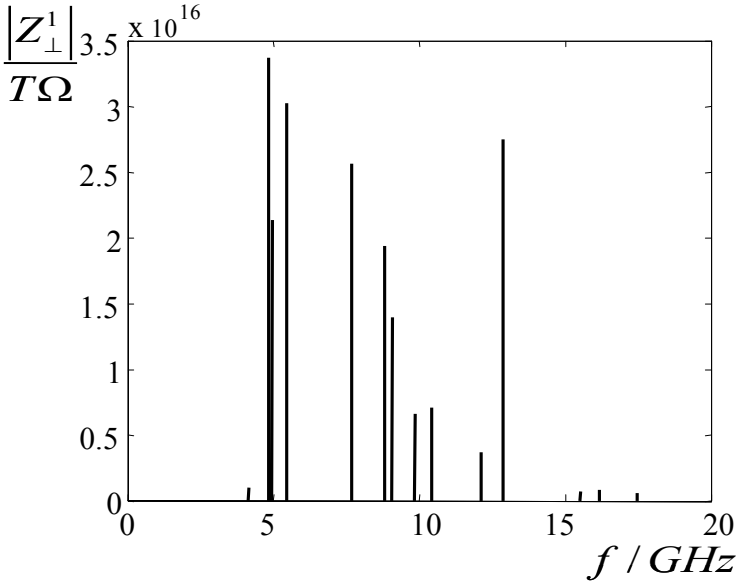

Fig 25. The transverse low-frequency impedance of LOLA.

Fig. 25 shows the frequencies and amplitudes used in Eq (13) to obtain wake function shown in Fig. 24 by dashed line. The values are obtained using the Prony-Pissarenko algorithm and are given in Table 4.

f_i, GHz	4.13	4.82	4.94	5.45	7.67	8.81	9.07
K_i, 10^{16}	0.10	3.37	2.13	3.02	2.56	1.94	1.39

f_i, GHz	9.85	10.4	12.1	12.87	15.5	16.2	17.4
K_i, 10^{16}	0.66	0.71	0.37	2.75	0.07	0.08	0.06

Table 4. The lowest frequencies and their amplitudes for long-range transverse wake function of 3rd harmonic section.

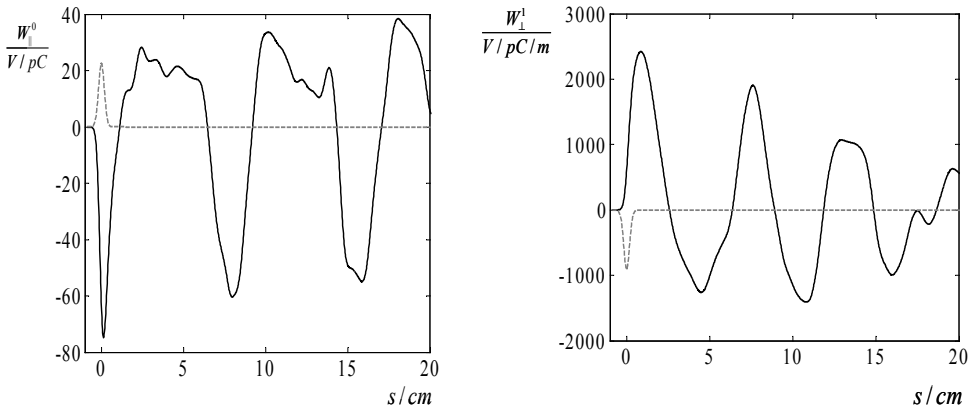

Fig 26. The longitudinal and transverse wake potentials for Gaussian bunch with $\sigma = 1.77\,mm$.

Fig. 26 shows the longitudinal and transverse wakes for Gaussian bunch

with $\sigma = 1.77mm$ as it can be a possible bunch length choice due to optimal compensation of non-linear distortion. The integral parameters for this case take values: energy loss – 52.9 V/pC, energy spread – 21.3 V/pC, transverse kick – 711 V/pC/m, kick spread – 533 V/pC/m.

6 DISCUSSION

The TESLA cavity is a main element of the LINAC and it is reasonable to compare the obtained wakes to ones of the TESLA cryomodule [8]:

$$w_{\parallel}^{cryo}(s) = -\theta(s)\cdot 41.5e^{-\sqrt{\frac{s}{1.74\cdot 10^{-3}}}} \quad \left[\frac{V}{pC\cdot m}\right],$$

$$w_{\perp}^{cryo}(s) = \theta(s)\left[121\left(1-\left(1+\sqrt{\frac{s}{0.92\cdot 10^{-3}}}\right)e^{-\sqrt{\frac{s}{0.92\cdot 10^{-3}}}}\right)\right] \quad \left[\frac{V}{pC\cdot m\cdot m}\right].$$

The above expressions are given on unit of active length and obtained for the case of infinite periodic structure (see [8] for details).

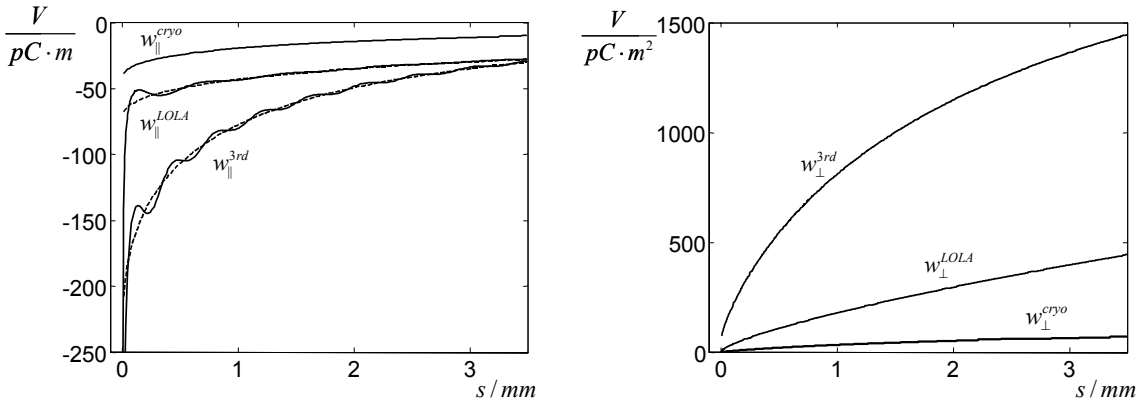

Fig 27. Comparison of the longitudinal and transverse wake functions for the cryomodule, the LOLA structure and the 3rd harmonic section.

The active length of the LOLA structure is $L_{total} = 3.64\ m$. And the normalized short range wake functions of the LOLA read

$$w_{\parallel}^{LOLA}(s) = -\theta(s)\left[70.8e^{-\sqrt{\frac{s}{3.96\cdot 10^{-3}}}} + 0.32\frac{\cos(1760s^{0.72})}{\sqrt{s}+1600s^{1.23}}\right] \quad \left[\frac{V}{pC\cdot m}\right],$$

$$w_{\perp}^{LOLA}(s) = \theta(s)\left[2804\left(1-\left(1+\sqrt{\frac{s}{11.7\cdot 10^{-3}}}\right)e^{-\sqrt{\frac{s}{11.7\cdot 10^{-3}}}}\right)+2530\sqrt{s}\right] \quad \left[\frac{V}{pC\cdot m\cdot m}\right].$$

The active length of the 3rd harmonic section is $L_{total} = 36\cdot 0.03844 = 1.3838\ m$. And the normalized short range wake functions of the section read

$$w_{\parallel}^{3rd}(s) = -\theta(s)\left[230e^{-\sqrt{\frac{s}{8.4\cdot 10^{-4}}}} + 0.65\frac{\cos(5830s^{0.83})}{\sqrt{s}+195s} + 0.026\delta(s)\right]\left[\frac{V}{pC\cdot m}\right],$$

$$w_{\perp}^{3rd}(s) = \theta(s)\left[1612\left(1-\left(1+\sqrt{\frac{s}{0.56\cdot 10^{-3}}}\right)e^{-\sqrt{\frac{s}{0.56\cdot 10^{-3}}}}\right)+3932\sqrt{s}+64\right] \quad \left[\frac{V}{pC\cdot m\cdot m}\right].$$

Fig. 27 shows comparison of the wake functions. The solid lines represent regular part of the functions and the dashed lines on the left figure correspond to the first term in the formulas and describe the behavior in infinite periodic geometry.

The increase of the wakes for the new elements comparing to the cryomodule can be explained by the reduced apertures of the new elements and the scaling law of the wakes [9]. If all dimensions of the structure are modified by the scaling factor λ the wakes scale as

$$w_{\parallel} \sim \lambda^{-2}, \qquad w_{\perp} \sim \lambda^{-3}.$$

The wake functions of the new elements include two terms. The first term describes behavior in an infinite periodic structure and plays the main role for long smooth bunches. The second term is caused by finite length of the structure and it is important for short or nonsmooth bunches.

The LOLA structure operates with bunches of the length $\sigma = 50\mu m$ and the second term in the wake expressions has to be taken into account. However, the 3rd harmonic section is used to linearize the energy-length correlation *before* the bunch compressor and therefore we are interested in bunch length of the order of 1mm. In this range the second term can be neglected and the effect of the step transition described by the third term in the wake expressions can be considered separately as it is shown in Fig. 28.

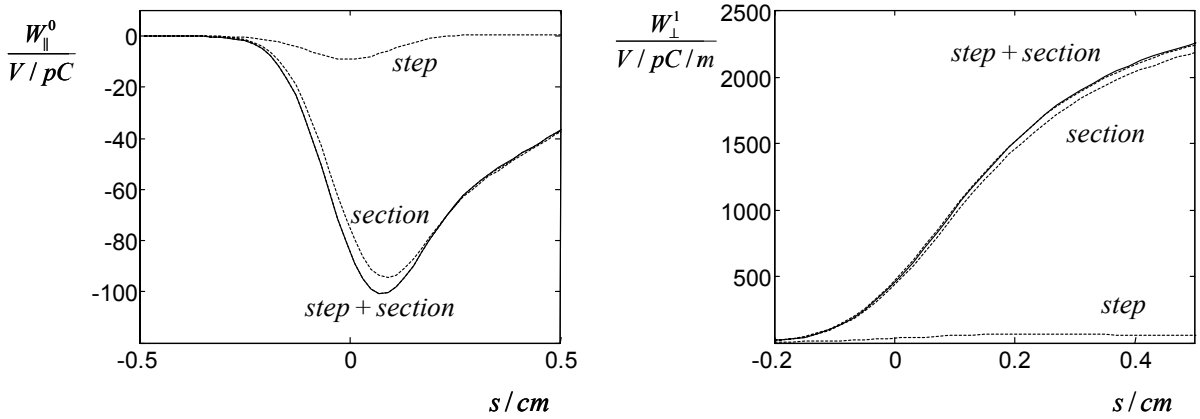

Fig 28. Comparison of the longitudinal and transverse wake potentials for step transition, the 3rd harmonic section without step transition and with it. The dashed curve describing the sum of the element effects is indistinguishable from the solid curve describing total structure effect.

Fig. 28 shows the wake potentials for Gaussian bunch with $\sigma = 1mm$. The wakes of the step transitions and the 3rd harmonic section without step transition are calculated separately and shown by dashed lines. Their sum is shown by dashed line too and is indistinguishable from the solid line presenting result of the direct simulation for the combined structure.

	loss, V/pC	energy spread, V/pC	kick,V/pC/m
step	6.41	2.65	31.7
section	64.95	27.84	520.3
section with step	71.39	28.84	542.1

Table 5. The integral parameters for step transition, the 3rd harmonic section without step transition and with it.

As shown in the Table 5 the effect of the step transition for smooth long bunch (Gaussian bunch with $\sigma = 1mm$) is below 10%.

CONCLUSION

The short- and long-range geometric wake fields of new elements to be installed in TTF-II are studied. The analytical forms of short- and long-range wake functions are obtained.

The numerical results confirm the theoretical estimations. The very short-range behavior of wake functions is dominated by one-cell term for the LOLA structure and by step transition term for the 3rd harmonic section.

ACKNOWLEDGEMENT

The authors would like to thank R. Schuhmann for providing a Matlab implementation of the Prony-Pisarenko method and N. Solyak for the geometry description of the 3rd harmonic section.

REFERENCES

[1] Zagorodnov I., Schuhmann R., Weiland T., *Long-time numerical computation of electromagnetic fields in the vicinity of a relativistic source*, J. Comp. Physics, 2003; **191**:525.

[2] Gluckstern R.L., *Longitudinal impedance of a periodic structure at high frequency*, Physical Review D. 1989; **39**(9):2780.

[3] Bane K.L.F et al., *Calculations of the short-range longitudinal wakefields in the NLC Linac*, SLAC-PUB-7862, 1998.

[4] Bane K., Sands M., *Wakefields of very short bunches in an accelerating cavity*, SLAC-PUB-4441, 1987.

[5] Zotter B.W., Kheifets S.A., *Impedances and Wakes in High-Energy Particle Accelerators*, World Scientific, London, 1997.

[6] Bane K.L.F., *Short-range dipole wakefields in accelerating structures for the NLC*, SLAC-PUB-9663, 2003.

[7] Parks, T.W., and C.S. Burrus, *Digital Filter Design*, John Wiley & Sons, 1987.

[8] Weiland T., Zagorodnov I., *The short-range transverse wake function for TESLA accelerating structure*, TESLA 2003-19, 2003.

[9] Bane K.L.F., *Wakefield effects in a linear collider*, SLAC-PUB-4169, 1986.